Materials Science & Engineering A 616 (2014) 155–160

Contents lists available at ScienceDirect

Materials Science & Engineering A

journal homepage: www.elsevier.com/locate/msea

Electron backscatter diffraction analysis of the crack development induced by uniaxial tension in commercially pure titanium

K. Tesař*, A. Jäger

Laboratory of Nanostructures and Nanomaterials, Institute of Physics, Na Slovance 2, Prague 182 21, Czech Republic

ARTICLE INFO

Article history:
Received 20 May 2014
Received in revised form
7 August 2014
Accepted 8 August 2014
Available online 19 August 2014

Keywords:
EBSD
Titanium alloys
Orientation relationships
Grain boundaries
Fracture
Phase transformation

ABSTRACT

Pure titanium with a duplex microstructure was used in this work to characterize the fracture mechanisms that occurred during quasi-static tensile loading at room temperature. The duplex microstructure was composed of α grains decorated by a small fraction of β phase along the grain boundaries and at triple junctions. Electron backscatter diffraction (EBSD) was performed to systematically characterize the crack development across approximately 10^3 grains. It has been found that the fracture mechanism involves both transgranular and intergranular cracking. Transgranular cracking is a much more common fracture mechanism. By comparing EBSD data with simulations, it was possible to denote the most probable crystallographic planes in hcp grains susceptible to transgranular cracking. Intergranular failure unambiguously prefers general grain boundaries, and all coincidence site lattice (CSL) boundaries are more resistant.

1. Introduction

Titanium and its alloys have been widely used in various applications due to their strength-to-weight ratio, biocompatibility and corrosion resistance. Commercially pure (CP) titanium provides very good corrosion resistance for its density and mechanical properties, and therefore it is a viable material for reaction vessels, parts affected by sea water and medical implants [1–3]. Titanium is an allotropic material in which transformation from the hexagonal close-packed (hcp) α phase to the body-centered cubic (bcc) β phase occurs at approximately 1156 K [1]. The precise transformation temperature depends on the concentration of impurities [1,4]. The effect of the cooling gradient and thermomechanical processing on the final microstructure and texture of the α→β→α transformation has been investigated in many works [1,5–8]. Furthermore, a strong dependence of the mechanical properties on the final microstructure has been shown [9–12].

Characterization of crack development in bulk materials plays an important role in determining possible failure. It has been shown that both microtexture and microstructure strongly influence fatigue-crack initiation [13–15]. A powerful technique for determining the grain orientation in a material is electron backscatter diffraction (EBSD). EBSD provides crystallographic orientation data across the inspected area with a high spatial resolution, down to 30 nm, and is capable of mapping large areas [16]. As a result, additional information such as the Schmid factors related to given slip systems, grain boundary characteristics and microtexture within the given specimen can be easily extracted [17,18].

Many studies have been performed on the relationship between the mechanical properties and the final microstructure [9–12], fatigue-crack development and the activation of various slip systems in CP titanium [17–20]. Despite a significant effort in this field, there is still an incomplete picture about crack propagation during mechanical loading. This deficiency follows from the complexity of Ti caused by its allotropic nature. In the present study, we statistically determine preferential sites for transgranular and intergranular cracks in duplex titanium grade 2 via EBSD.

2. Experimental details

The commercially pure titanium rods, ASTM grade 2, with a 16 mm diameter used for this study were provided by Baoji Titanium Industry Co., Ltd. The extruded rods were supplied in an annealed condition, and the composition is given in Table 1. Both microstructural and tensile specimens were cut along a plane parallel to the extrusion direction by electrical-discharge machining. Thereafter, the specimens were heat-treated in an argon atmosphere at a heating rate of 0.2 K/s up to 1173 K, held for 1 h and, subsequently, cooled to room temperature in argon at a cooling rate of 5 K/s.

* Corresponding author. Tel.: +420 721 869 628.
E-mail address: tesarkar@fzu.cz (K. Tesař).

http://dx.doi.org/10.1016/j.msea.2014.08.028

Table 1
Chemical composition of as-received titanium grade 2.

Element	Fe	C	N	O	H	Residual	Ti
Content (wt%)	0.15	0.02	0.03	0.15	0.001	< 0.4	Balance

Flat tensile specimens with gauge dimensions of $15 \times 6 \times 3\ mm^3$ were deformed on an Instron 5882 at room temperature (RT) and at an initial strain rate of $10^{-3}\ s^{-1}$. Specimens for subsequent EBSD analysis were deformed to 10% elongation to obtain narrow cracks instead of complete failure, which would occur with greater deformation. This enabled us to obtain EBSD maps on both sides of the propagating cracks and to more easily link the originally neighboring microstructural features. If a link of two opposite grains or lattices was disputable, this couple was omitted from further evaluation.

Specimens for light microscopy and EBSD were mechanically polished using SiC paper up to 2400 grit, and they were then polished with a solution of colloidal silica followed by ion milling (for EBSD) or chemical etching (for light microscopy). EBSD measurements were performed using a FEI Quanta 3D FEG scanning electron microscope fitted with a TSL/EDAX Hikari camera. To obtain reasonable statistics for crack evaluation, a total of 49 EBSD maps was measured, each referring to a single crack. A total of $\sim 10^3$ grains was considered. The EBSD measurements were performed in the plane given by the extrusion direction (ED) and the transverse direction (TD). A plane of EBSD mapping was perpendicular to the nominal crack propagation direction. Specimen preparation was optimized to reach a plane near the tip of a propagating crack and thus the morphology of the crack in the bulk material was investigated. The mapping step for EBSD was 1 or 2 μm, depending on the required resolution near the considered crack.

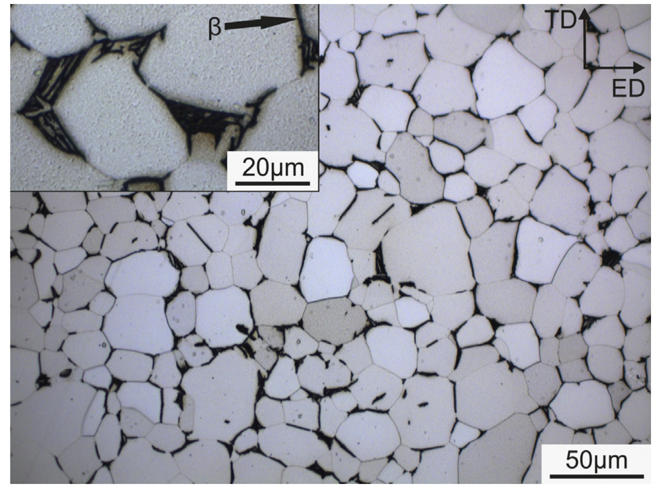

Fig. 1. Typical microstructure of the Ti grade 2 investigated in this work. The hcp α grains (light) and bcc β phase regions (dark) after heat treatment (1173 K/1 h) are shown by light microscopy; the inset shows a detail of the α–β lamellar morphology at triple junctions and grain boundaries.

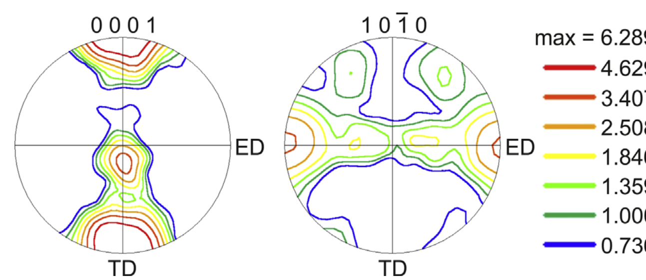

Fig. 2. Texture of the specimen after the heat treatment calculated from EBSD data. ED – extrusion direction and TD – transverse direction. The color coding depicts the calculated intensity. (For interpretation of the references and color in this figure legend, the reader is referred to the web version of this article.)

3. Results and discussion

3.1. Microstructural characterization

The as-received material was composed of equiaxed α-phase grains with an average grain size of 9 μm (linear-intercept method). A heat-treatment procedure was optimized to obtain a duplex α+β microstructure, common in some titanium alloys with β-phase stabilizing elements [21]. Dobeson et al. [22] pointed out that the α-to-β transformation of titanium grade 2 initiates at a temperature of 1143 K and develops gradually over a certain temperature interval. This offers an opportunity to interrupt the transformation and to achieve the required microstructure. Fig. 1 shows the duplex α+β microstructure investigated in this work, which was obtained by annealing the specimen at a temperature of 1173 K for 1 h. Neither the time nor the temperature was sufficient to fully transform the hcp α phase to the bcc β phase in the entire specimen. This led to the formation of the β phase at sites with the lowest free energy, such as grain boundaries and triple junctions. Dheda et al. [21] explained the presence of the β phase at grain boundaries as a result of segregation of the β stabilizing Fe, and our results support this conclusion. The average α grain size of a specimen after heat treatment (1173 K/1 h) determined by the linear-intercept method was 37 μm.

It is well known that the volume ratio of α/β phases in the specimen can change significantly after only a small alteration of the heat-treatment procedure [23]. In triple junctions that have a larger volume of the β phase, it is possible to observe a transformed α-lamellar microstructure (inset of Fig. 1). This is typical for α→β→α transformations with fast or intermediate cooling rates [24,25]. The morphology of this lamellar microstructure depends on the cooling gradient [24,25]. Provided that the α-to-β transformation is completed in the entire specimen, and cooling rate would be equivalent to, or even faster than, the cooling rate used in this work, the lamellar microstructure would be a dominant feature in the entire specimen.

The texture of the material after heat treatment is shown in Fig. 2. Direct pole figures in the (0 0 0 1) and $\{10\bar{1}0\}$ planes calculated from EBSD data show that the basal planes tend to be oriented parallel with the ED. This is in agreement with other works [26]. The plots depict the preferred orientation of grains within the inspected areas in ED–TD plane and they are calculated from $\sim 10^4$ grains.

3.2. Tensile tests

Fig. 3a shows the engineering stress–strain curve measured under tension at RT for the microstructure in Fig. 1. The characteristic values of the ultimate tensile strength σ_{max}, yield strength σ_{02} and elongation to failure A calculated from this curve are also shown there. Although the stress–strain curve does not indicate any cracking before approximately 17% plastic strain, it has been observed that tensile deformation causes the formation of many parallel cracks. It is important to mention that these cracks emerged gradually during the tensile straining and that the first cracking could be visually detected at approximately 7% plastic strain. The typical morphology of cracks at 10% plastic strain is shown in Fig. 3b. A characteristic feature of these cracks is that